

Small signal stability and dynamic performance investigation on multi-machines power system including DFIG wind farm

Khaled Kouider, Abdelkader Bekri

The Control, Analysis and Optimization of the Electro-Energetic Systems (CAOSEE) Laboratory, Tahri Mohamed University, Bechar, Algeria

Article Info

Article history:

Received Oct 23, 2019

Revised Mar 15, 2023

Accepted Mar 29, 2023

Keywords:

DFIG

Electromechanical oscillations

Power system stability

PSAT

Wind power

WSCC

ABSTRACT

The boundless potential of wind power in augmenting global energy production is a promising prospect. The efficient design and cost-effectiveness of doubly fed induction generator (DFIG) wind systems make them an optimistic solution for incorporating wind power on a massive scale. However, integrating these systems into power grids poses several challenges, including power system stability. This study examines the small signal stability and dynamic performance of a modified Western System Coordinating Council (WSCC) 9-bus system including a DFIG wind farm using load flow analysis, and both electromechanical oscillations and eigenvalue analysis. Three case studies were conducted based on the DFIG location and power increment. The simulation is carried out with the aid of the power system analysis toolbox (PSAT) that operates within the MATLAB environment. The study's findings suggest that the perturbation and location of the DFIG relative to the system's load have a minimal influence on the overall system's stability and efficiency. However, when considering damping ratio, power angle, and rotor speed deviations, generators 1 and 2 with the perturbed DFIG installed on bus 8 are the most sensitive units to instability. Hence, larger perturbations and different DFIG's location influence on power systems necessitates further analysis.

This is an open access article under the [CC BY-SA](https://creativecommons.org/licenses/by-sa/4.0/) license.



Corresponding Author:

Khaled Kouider

The Control, Analysis and Optimization of the Electro-Energetic Systems (CAOSEE) Laboratory

Tahri Mohamed University

Street of Independence, BP 417, Bechar, Algeria

Email: khouiledkhaled@gmail.com

1. INTRODUCTION

Rising concerns about the fossil fuels' environmental impact have led to an increased focus on exploring renewable energy as a viable alternative. The accuracy and sustainability of wind turbines increase in proportion to their level of penetration. Wind farms must be able to consistently generate the required amount of electricity based on the current wind speed level and the demands of the grid [1]. Doubly fed induction generator (DFIG) wind power technologies are recognized as one of the most sophisticated solutions in this field due to their high efficiency compared to cost. However, the power system's stability could be significantly compromised in the event of a lack of control and weak damping.

In heuristic terms, power system stability pertains to the capacity of a power system to sustain a state of equilibrium during regular operation and to attain a satisfactory equilibrium state following an external dis-

turbance. Power system instability can arise from various factors, including unsynchronized rotating inertias, low voltage, faults resulting from natural causes, or malfunctioning of protection system devices. Power system's stability is reliant on three crucial aspects, specifically, voltage stability, frequency stability, and rotor angle stability. This field has been extensively researched. Particular concept in this area extensively reviewed in [2]. Asija *et al.* [3] conducted a contingency analysis and power flow study of the Western System Coordinating Council (WSCC) 9-bus power system using MATLAB, while Eremia and Shahidehpour [4] present a detailed analysis of power system dynamics and stability concepts.

DFIG wind systems have recently emerged as a prominent trend in wind power conversion technologies, primarily because of their considerable influence on power system stability. Rosyadi *et al.* [5] has produced a variable speed wind turbine (VSWT) generator model that is simplified and intended for use in dynamic simulation examination. Abo-Khalil [6] conducted a thorough examination of how wind farms affect the power systems' stability, considering the incorporation of sustainable energy supply. Ngamroo [7] carried out a comprehensive and in-depth analysis of the DFIG's effect on the power systems' dynamic performance by reviewing the literature thoroughly. The review comprehensively covered a wide range of topics, such as various modeling techniques, control strategies, and their potential impacts the stability.

The preservation of power system equilibrium is critical, and small signal stability plays a vital role in it. In this context, a comparison was made between DFIG and squirrel-cage induction generator (SCIG) turbines in an IEEE 14-bus system, as investigated by [8]. Analogies with static VAR compensators (SVC) and shunt static synchronous compensator (STATCOM) have been introduced into DFIG-based turbines for small signal stability enhancement purposes [9]. The of DFIG's based turbines effect on power systems' voltage stability was scrutinized by [10], with results showing that stability can only be sustained by small-scale wind power penetration. As wind energy integration continues to affect power systems, researchers have put forward different approaches to enhance small signal stability. In their work, Gibbard *et al.* [11] delved into the intricacies of power system control, small-signal stability, and dynamic performance, paying particular attention to the crucial role of incorporating wind energy integration into the analysis of power system reliability. On a related topic, Dasu *et al.* [12] recommended the whale optimization algorithm for this purpose in a substantial power system.

The study of power system oscillations is a crucial aspect of power system stability, given its considerable influence on the dependability and security of these systems. Such oscillations can be attributed to a range of factors, including torque imbalances, insufficient damping, poor controller tuning, and interactions between controllers and series capacitor compensated lines [2], [4]. Electromechanical oscillations, which are among the most dominant modes of power oscillations, can be categorized into two sorts: local and inter-area modes. Local modes of electromechanical oscillations typically manifest at frequencies ranging from 0.7-2 Hz, while inter-area modes tend to occur at frequencies between 0.1-0.8 Hz, as documented in [13]-[15]. Furthermore, The integration of renewable energy, including wind energy, into conventional grids can pose challenges to power system oscillations damping, as highlighted in a recent bibliographic review by [16]. Ghosh and Senroy [17] delves into the localized nature of electromechanical oscillations in power systems by exploring how local factors, such as generator damping and system topology, affect the oscillations. According to [18], low-frequency oscillations in power systems have a strong mathematical and analytical basis, and wide-area monitoring and control systems can play a key role in their control and regulation.

This paper investigates the small signal stability and dynamic behavior of a multi-machine power system that includes a DFIG wind farm located at various locations within the WSCC 9-bus system. Then, we assess it's efficiency using the PSAT Toolbox. The research is categorized into four parts, beginning with an introduction that outlines the stability statement. In the second segment, the tested system is mathematically modeled, with a focus on describing the wind farm. In the third part, the power system analysis toolbox (PSAT) model used for the simulation is exhaustively described. Finally, the fourth portion provides a comprehensive interpretation of the simulation findings, including the machine's influence on the system's dynamic behavior and stability.

2. SYSTEM MODELING

The synchronous machine's dynamic models adequate for stability studies are well-reviewed in [2], [19]. In this passage, we will focus only on DFIG modeling. The typical schematic of the DFIG based wind turbine connected to the grid with the back-to-back converter is well drawn in Figure 1.

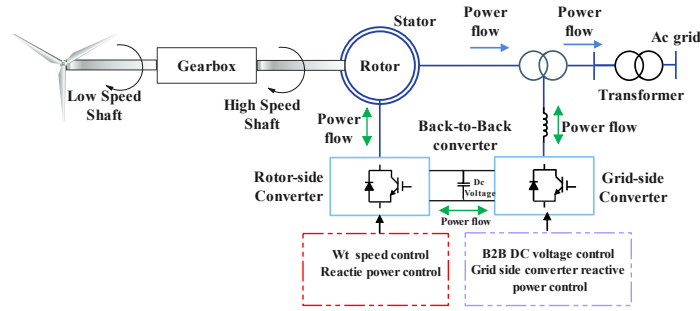


Figure 1. The standard configuration of a grid-connected DFIG wind system

2.1. DFIG dynamic modeling

The mathematical modeling of the DFIG based wind turbine, including its related electrical equations, has been explicated in great depth in [20], [21]. To build upon this foundation, our study employs the comprehensive system of equations established in [22], [23]. Hence, for the stator windings:

$$v_{ds} = (x_s + x_m) i_{qs} + x_m i_{qr} - R_s i_{ds} \quad (1)$$

$$v_{qs} = -(x_s + x_m) i_{ds} + x_m i_{dr} - R_s i_{qs} \quad (2)$$

and for the rotor:

$$v_{dr} = -(1 + \omega) ((x_r + x_m) i_{qr} + x_m i_{qs}) - R_r i_{dr} \quad (3)$$

$$v_{qr} = -(1 - \omega) ((x_r + x_m) i_{dr} + x_m i_{ds}) - R_r i_{qr} \quad (4)$$

where $v_{dr}, v_{qr}, v_{ds}, v_{qs}$, are dq components of the rotor and stator voltages. The dq currents for both stator and rotor currents are given by $i_{ds}, i_{qs}, i_{dr}, i_{qr}$. R_r, R_s are the rotor and stator resistances. x_r, x_s, x_m rotor, stator, and mutual inductances. ω is the rotor speed. As a result, it is possible to represent the electromagnetic torque using (5).

$$T_e = x_m (i_{qr} i_{qs} - i_{ds} i_{dr}) \quad (5)$$

Furthermore, the powers are expressed in the following manner:

$$P_s = v_{ds} i_{ds} + v_{qs} i_{qs} \quad (6)$$

$$Q_s = v_{qs} i_{ds} - v_{ds} i_{qs} \quad (7)$$

$$P_r = v_{dr} i_{dr} + v_{qr} i_{qr} \quad (8)$$

$$Q_r = v_{qr} i_{dr} - v_{dr} i_{qr} \quad (9)$$

Finally, the total power exchanged with the grid:

$$P_{tot} = P_s + P_r \quad (10)$$

$$Q_{tot} = Q_s + Q_r \quad (11)$$

when utilizing the vector control technique, the rotor decouples both active and reactive powers. We assume that the active power directly affected by the q component, Whereas i_{dr} regulates the reactive power. Accurate calculation of the limits for rotor currents is an indispensable requirement to achieve DFIG's optimal steady-state operation:

$$i_{qr_{max}} \approx -\frac{x_s + x_m}{x_m} P_{min} \quad (12)$$

$$i_{qr_{min}} \approx -\frac{x_s + x_m}{x_m} P_{max} \quad (13)$$

$$i_{dr_{max}} \approx -\frac{x_s + x_m}{x_m} Q_{min} - \frac{x_s + x_m}{x_m^2} \quad (14)$$

$$i_{dr_{min}} \approx -\frac{x_s + x_m}{x_m} Q_{max} - \frac{x_s + x_m}{x_m^2} \quad (15)$$

3. THE SIMULATION MODEL DESCRIPTION

In the actual work, The WSCC 9-bus power system [24] with (100 MVA, 60 Hz base) is employed. This model comprises three synchronous generators correlated to buses 1, 2, and 3 (bus 1 is the slack bus, 2 and 3 are PV buses). Three PQ loads bus attached to buses 5, 6, and 8, six transmission lines connect the aforementioned components to the remaining system, as exhibited in Figure 2. The data employed in the simulation are listed on the supplementary file. The WSCC test model is modified by integrating the DFIG wind farm in different locations at load buses as mentioned in Figure 3, taking into account that, the first case represents DFIG at bus 5, the second case at bus 6 and, the last case is when the wind farm is coupled at bus 8. The simulations are performed using the PSAT toolbox. It is a free toolbox used for load flow studies and stability analysis compatible with the MATLAB platform [25]. In the three cases, the DFIG wind farm with unity power factor with 0.5 p.u. generation power is attached and subjected to a 0.25 p.u. power increment at ($t = 100$ s) and lasts to the end of the simulation.

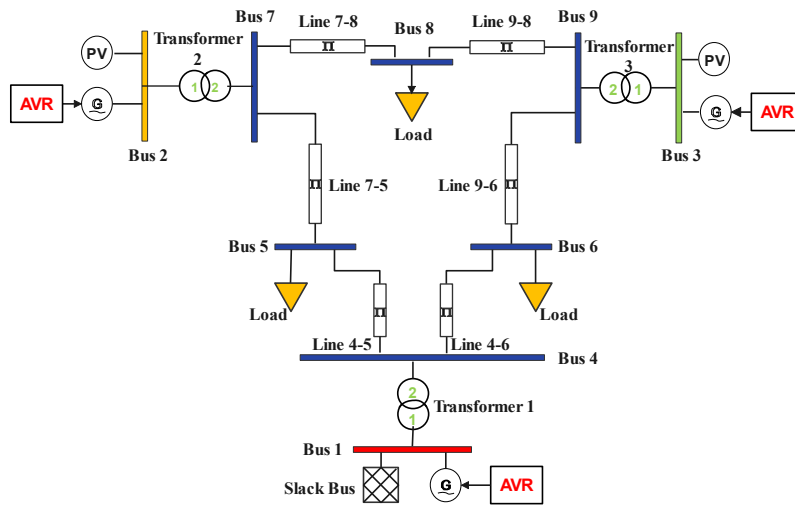


Figure 2. WSCC 9-bus test system in PSAT

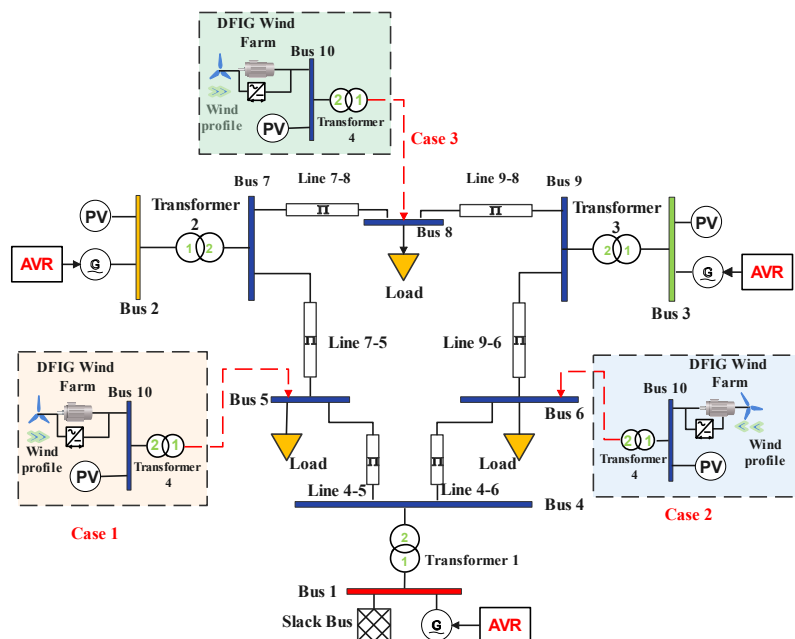


Figure 3. Modified WSCC 9-bus test system including the three cases

4. ANALYSIS OF SIMULATION FINDINGS

The time-domain simulation are well drawn by Figures 4 and 5, which was performed using the trapezoidal integration method. This method is known for its robustness and stability across various test cases. Notably, power augmentation was achieved through the use of a perturbation file that was created and imported into the PSAT toolbox using MATLAB programming skills. The following five sub-sections will examine the discussion of these results.

4.1. Power angle deviation

The power angle deviation has the potential to involve the power system’s stability, which influences the synchronism of generator rotors. The power angle evolution is well depicted in Figure 4, where the injection of 0.25 p.u. of wind power by the DFIG causes δ_1 , δ_2 , and δ_3 to deviate by 20.3° , 22.5° , and 15.6° in the three cases, respectively. The third case has the highest relative angle deviation in $\Delta\delta_{1-2}$ and $\Delta\delta_{1-3}$ with 1.5° and 1.38° as established by Figures 4(a) and 4(b) in that order. Moreover, the maximum peak for $\Delta\delta_{2-3}$ was observed in case 2 with 0.5° , as presented in Figure 4(c). While not necessarily alarming, a 1.5 degree relative power angle deviation necessitates careful monitoring and measures to ensure the stable and reliable operation between generators.

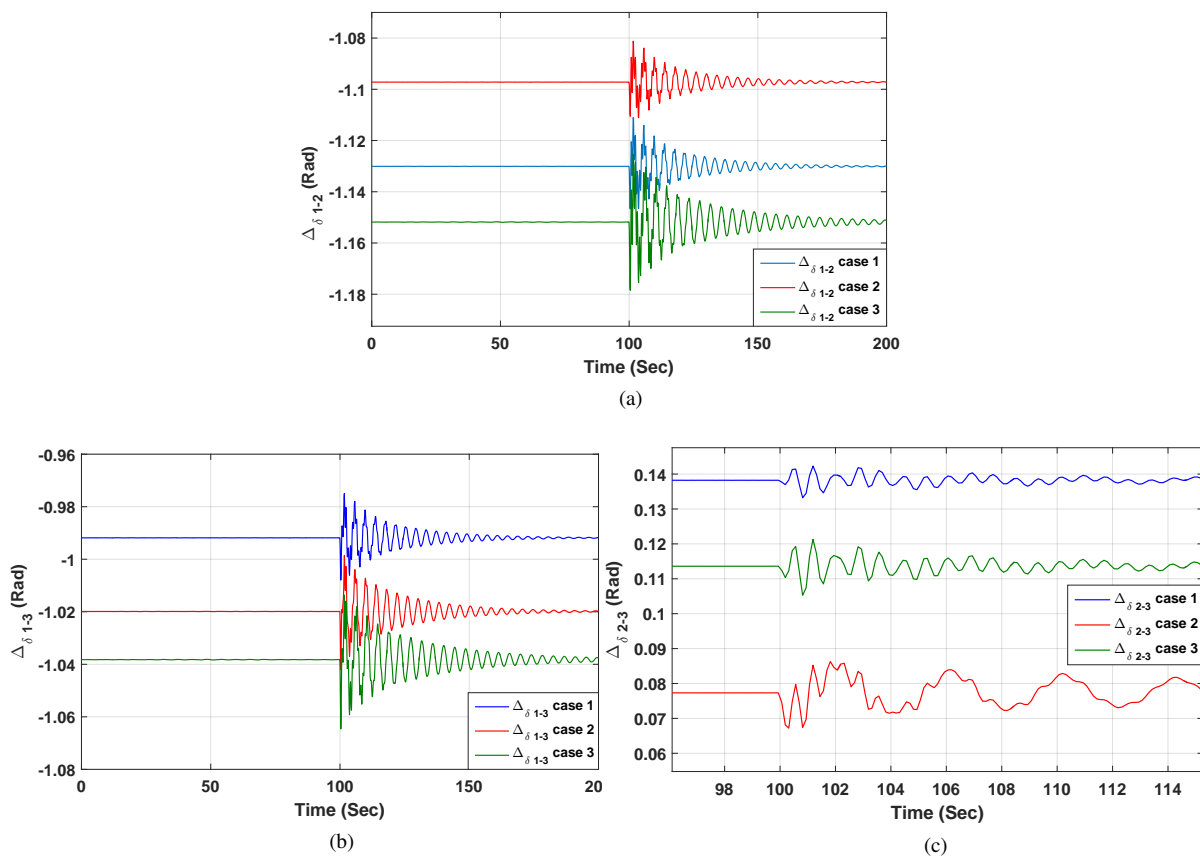


Figure 4. Power angle deviation (a) $\Delta\delta_{1-2}$, (b) $\Delta\delta_{1-3}$, (c) $\Delta\delta_{2-3}$

4.2. Generators speed deviation

The generator speeds deviation are accurately displayed in Figure 5. Before the power increment, the fluctuations of the generators’ speeds (frequency) for all cases precisely oscillate around 0 p.u. Similar to the angle deviation, the highest relative deviation in rotor speed is observed in case 3, with 0.038% for $\Delta\omega_{syn1-2}$ and 0.03% for $\Delta\omega_{syn1-3}$, as shown in Figures 5(a) and 5(b), respectively. On the other hand, Figure 5(c) exhibits the maximum deviation for $\Delta\omega_{syn2-3}$ on case 2 with 0.023% following the power addition. Moreover, instant

oscillations, spanning a scope of $\pm 0.025\%$, emerge and gradually diminish in magnitude, provided that the overall stability of the system is not intensely compromised.

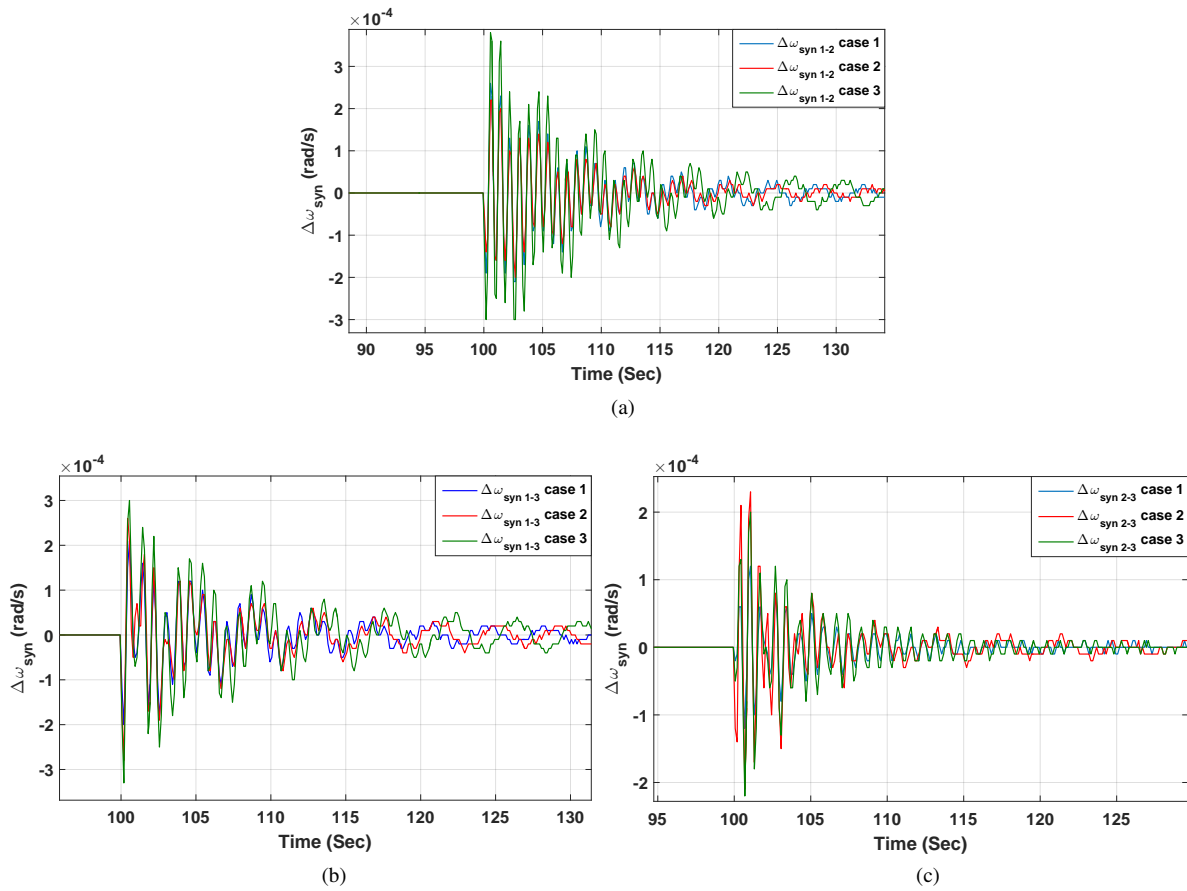


Figure 5. The generators speed variation (a) $\Delta\omega_{syn1-2}$, (b) $\Delta\omega_{syn1-3}$, (c) $\Delta\omega_{syn2-3}$

4.3. Bus voltages

The voltages V_1, V_2, V_3, V_5, V_6 and V_8 are summarized in Table 1. Thus, it can be assumed that at $t = 100$ s, the bus voltages remained in close alignment with the given references. $V_{bus 5}$ in the 3rd case gets the maximum over-undershoots within the range of $+0.45\%$ to -0.48% . Furthermore, it was found that there was no requirement for reactive power compensation (voltage regulation) in all instances, indicating that the power system was able to effectively manage the voltage levels, even with changes in power output from the DFIG.

Table 1. Detailed data of the bus voltages V_1, V_2, V_3, V_5, V_6 , and V_8

	$V_{bus 1}$			$V_{bus 2}$			$V_{bus 3}$		
	Value	Over (%)	Under (%)	Value	Over (%)	Under (%)	Value	Over (%)	Under (%)
Case 1	1.04	0.09	-0.09	1.25	0.19	-0.19	1.25	0.19	-0.19
Case 2	1.04	0.09	-0.09	1.25	0.29	-0.29	1.25	0.19	-0.19
Case 3	1.04	0.19	-0.19	1.25	0.29	-0.39	1.25	0.29	-0.39
	$V_{bus 5}$			$V_{bus 6}$			$V_{bus 8}$		
	Value	Over (%)	Under (%)	Value	Over (%)	Under (%)	Value	Over (%)	Under (%)
Case 1	1.015	0.19	-0.09	1.017	0.19	-0.19	1.019	0.29	-0.19
Case 2	0.9973	0.2	-0.25	1.028	0.09	-0.19	1.018	0.19	-0.29
Case 3	0.9909	0.45	-0.48	1.009	0.39	-0.39	1.026	0.38	-0.39

4.4. Load flow results

Detailed information about the load flow can be found in Tables 2 and 3. The negative phases on buses 4, 5, and 6 denote that voltages' phase of these buses lag from the reference phase 0°. Hence, the power increment at $t = 100$ s, for different locations of the DFIG wind farm on system loads, has a minimal impact on the generators' power and voltage, and the system's load flow. However, the negative reactive power losses from Table 3 denote an excessive generation in this power resulted in voltage rise, which should be monitored and assessed for reliable operation. Despite this, the findings suggest that the system can handle the power increase with negligible influence on its functioning.

Table 2. Load flow results after power increment (at $t = 100$ s)

	Case 1			Case 2			Case 3		
	V [p.u.]	Phase [rad]	P_{gen} [p.u.]	V [p.u.]	Phase [rad]	P_{gen} [p.u.]	V [p.u.]	Phase [rad]	P_{gen} [p.u.]
Bus 1	1.040	0.35534	0.21564	1.04	0	0.21711	1.04	0	0.24105
Bus 2	1.025	0.56939	1.63	1.025	0.20507	1.63	1.025	0.25006	1.63
Bus 3	1.025	0.47972	0.85	1.025	0.13543	0.85	1.025	0.16576	0.85
Bus 4	1.0318	0.34371	0	1.0287	-0.01169	0	1.0222	-0.01306	0
Bus 5	1.0154	0.3482	0	0.99728	-0.03696	0	0.99085	-0.02284	0
Bus 6	1.0169	0.32391	0	1.0278	2e-5	0	1.009	-0.01825	0
Bus 7	1.0306	0.47279	0	1.0269	0.10813	0	1.0287	0.15329	0
Bus 8	1.0195	0.41689	0	1.018	0.06063	0	1.0261	0.11921	0
Bus 9	1.0343	0.43271	0	1.0356	0.08848	0	1.0348	0.11879	0
Bus 10	1.03	0.42897	0.5	1.03	0.08065	0.5	1.03	0.19989	0.5

Table 3. Total generation, load, and losses after power increment (at $t = 100$ s)

	Total generation		Total load		Total losses	
	P_{gen}	Q_{gen}	P_{load}	Q_{load}	P_{loss}	Q_{loss}
Case 1	3.1956	0.04628	3.15	1.15	0.04564	-1.1037
Case 2	3.1971	0.06433	3.15	1.15	0.04711	-1.0857
Case 3	3.2211	0.17691	3.15	1.15	0.07105	-0.9730

4.5. Eigenvalue analysis

This experiment utilized the eigenvalue analysis tool that is available in the PSAT toolbox. A total of 29 states were initiated and analyzed, which included 10 pairs of complex states. The analysis revealed that the system is stable, as evidenced by the results displayed in Figure 6. Eigenvalues analysis is crucial for assessing the stability of a linearized power system model by identifying its Eigenvalues. Based on Table 4, local mode oscillations are detected on the three synchronous generators, each with varying damping ratios. The proximity of pseudo-frequency to the system frequency suggests low damping, which can cause oscillations with decaying amplitudes. Generators 1 and 2 have the most critical modes with poor damping of 2.1% and 2%, respectively, making them more prone to instability from perturbations. Therefore, critical modes should receive particular attention, as they have the potential to cause instability if not damped properly. This highlights the significance of identifying and damping critical modes in power system stability analysis and control.

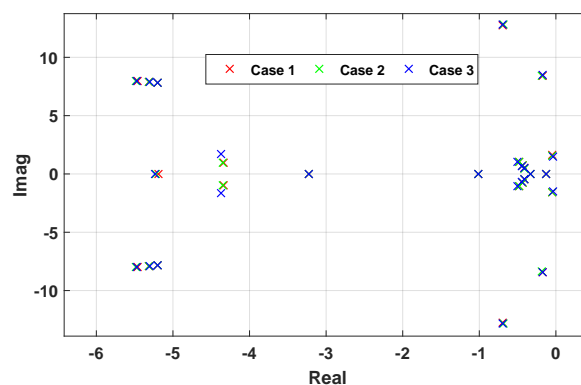


Figure 6. The standard configuration of a grid-connected DFIG wind system

Table 4. Eigenvalues analysis detailed report

	Eigenvalues	Most Associated States	Eigenvalues		Frequency	Oscillation Mode
			Real Part	Img Part		
Case 1	Eig As # 4	delta.Syn_3, omega.Syn_3	-0.69532	12.7752	2.0362	Local Mode 3
	Eig As # 5	delta.Syn_3, omega.Syn_3	-0.69532	-12.7752	2.0362	Local Mode 3
	Eig As # 6	delta.Syn_2, omega.Syn_2	-0.17424	8.4129	1.3392	Local Mode 2
	Eig As # 7	delta.Syn_2, omega.Syn_2	-0.17424	- 8.4129	1.3392	Local Mode 2
	Eig As #17	delta.Syn_1, omega.Syn_1	-0.04414	1.6036	0.25532	Local Mode 1
	Eig As #18	delta.Syn_1, omega.Syn_1	-0.04414	- 1.6036	0.25532	Local Mode 1
		Eigenvalues	Most Associated States	Eigenvalues		Frequency
			Real Part	Img Part		
Case 2	Eig As # 4	delta.Syn_3, omega.Syn_3	-0.68553	12.8079	2.0414	Local Mode 3
	Eig As # 5	delta.Syn_3, omega.Syn_3	-0.68553	- 12.8079	2.0414	Local Mode 3
	Eig As # 6	delta.Syn_2, omega.Syn_2	-0.18118	8.3843	1.3347	Local Mode 2
	Eig As # 7	omega.Syn_2, delta.Syn_2	-0.18118	- 8.3843	1.3347	Local Mode 2
	Eig As #17	omega.Syn_1, delta.Syn_1	-0.04268	1.5628	0.24882	Local Mode 1
	Eig As #18	delta.Syn_1, omega.Syn_1	-0.04268	- 1.5628	0.24882	Local Mode 1
		Eigenvalues	Most Associated States	Eigenvalues		Frequency
			Real Part	Img Part		
Case 3	Eig As # 4	omega.Syn_3, delta.Syn_3	-0.96248	12.8007	2.0403	Local Mode 3
	Eig As # 5	delta.Syn_3, omega.Syn_3	-0.96248	-12.8007	2.0403	Local Mode 3
	Eig As # 6	delta.Syn_2, omega.Syn_2	-0.17492	8.4582	1.3464	Local Mode 2
	Eig As # 7	delta.Syn_2, omega.Syn_2	-0.17492	-8.4582	1.3464	Local Mode 2
	Eig As #17	omega.Syn_1, delta.Syn_1	-0.03192	1.4917	0.23746	Local Mode 1
	Eig As #18	omega.Syn_1, delta.Syn_1	-0.03192	-1.4917	0.23746	Local Mode 1
				Real Part	Img Part	

5. CONCLUSION

Based on the findings of this study, it is evident that the placement of a DFIG-based wind turbine at load buses does not significantly affect the stability and performance of the WSCC 9-bus power system. The load flow report demonstrated the system's ability to maintain its controlled operating values during perturbations, and eigenvalue analysis showed that the system remained stable as long as the electromechanical oscillations were well-damped. However, particular attention should be paid to the behavior of these oscillations in the face of larger perturbations and different DFIG locations, may exert a considerably more potent influence on the system's stability and performance.




REFERENCES

- [1] S. Simani and S. Farsoni, "Introduction," *Fault Diagnosis and Sustainable Control of Wind Turbines*, Oxford, UK: Butterworth-Heinemann, 2018, pp. 1-12.
- [2] P. Kundur, *Power System Stability and Control*, New York, NY, USA: McGraw-Hill, 1994.
- [3] D. Asija, P. Choudekar, K. M. Soni, and S. K. Sinha, "Power flow study and contingency status of WSCC 9 Bus test system using MATLAB," in *2015 International Conference on Recent Developments in Control, Automation and Power Engineering (RDCAPE)*, 2015, pp. 338-342, doi: 10.1109/RDCAPE.2015.7281420.
- [4] M. Eremia and M. Shahidehpour, *Handbook of Electrical Power System Dynamics: Modeling, Stability, and Control*, Hoboken, NJ, USA: John Wiley & Sons, 2013.
- [5] M. Rosyadi, A. Umamura, R. Takahashi, J. Tamura, N. Uchiyama, and K. Ide, "Simplified model of variable speed wind turbine generator for dynamic simulation analysis," *IEEJ Transactions on Power and Energy*, vol. 135, no. 9, pp. 538-549, 2015, doi: 10.1541/ieejpes.135.538.
- [6] A. G. Abo-Khalil, "Impacts of wind farms on power system stability," in *Modeling and Control Aspects of Wind Power Systems*, S. M. Mueen, A. Al-Durra, and H. M. Hasanien, Eds., London, UK: InTech, 2013.
- [7] I. Ngamroo, "Review of DFIG wind turbine impact on power system dynamic performances," *IEEJ Transactions on Electrical and Electronic Engineering*, vol. 12, no. 3, pp. 301-311, 2017, doi: 10.1002/tee.22379.
- [8] D. R. Chandra *et al.*, "Impact of SCIG, DFIG wind power plant on IEEE 14 bus system with small signal stability assessment," in *2014 Eighteenth National Power Systems Conference (NPSC)*, 2014, pp. 1-6, doi: 10.1109/INDICON.2014.7030424.
- [9] S. Bagchi, S. Goswami, R. Bhaduri, M. Ganguly, and A. Roy, "Small signal stability analysis and comparison with DFIG incorporated system using FACTS devices," in *2016 IEEE 1st International Conference on Power Electronics, Intelligent Control and Energy Systems (ICPEICES)*, 2016, pp. 1-5, doi: 10.1109/ICPEICES.2016.7853294.
- [10] S. Pérez-Londoño, L. Rodríguez-García, and Y. U. López, "Effects of doubly fed wind generators on voltage stability of power systems," in *2012 Sixth IEEE/PES Transmission and Distribution: Latin America Conference and Exposition (T&D-LA)*, 2012, pp. 1-6, doi: 10.1109/TDC-LA.2012.6319119.
- [11] M. Gibbard, P. Pourbeik, and D. Vowles, *Small-signal stability, control and dynamic performance of power systems*, Adelaide, Australia: The University of Adelaide Press, 2015, pp. 1-22.




- [12] B. Dasu, S. Mangipudi, and S. Rayapudi, "Small signal stability enhancement of a large scale power system using a bio-inspired whale optimization algorithm," *Protection and Control of Modern Power Systems*, vol. 6, pp. 35-45, Jan. 2021, doi: 10.1186/s41601-021-00215-w.
- [13] M. Klein, G. J. Rogers, and P. Kundur, "A fundamental study of inter-area oscillations in power systems," *IEEE Transactions on Power Systems*, vol. 6, no. 3, pp. 914-921, 1991, doi: 10.1109/59.119229.
- [14] S. Avdakovic, A. Nuhanovic, M. Kusljagic, E. Becirovic, and M. Music, "Identification of low frequency oscillations in power system," in *2009 International Conference on Electrical and Electronics Engineering - ELECO 2009*, 2009, pp. I-103-I-107, doi: 10.1109/ELECO.2009.5355325.
- [15] L. Yang, Z. Xu, J. Østergaard, Z. Y. Dong, K. P. Wong, and X. Ma, "Oscillatory Stability and Eigenvalue Sensitivity Analysis of A DFIG Wind Turbine System," *IEEE Transactions on Energy Conversion*, vol. 26, no. 1, pp. 328-339, 2011, doi: 10.1109/TEC.2010.2091130.
- [16] Z. Rafique, H. M. Khalid, S. M. Muyeen, and I. Kamwa, "Bibliographic review on power system oscillations damping: An era of conventional grids and renewable energy integration," *International Journal of Electrical Power & Energy Systems*, vol. 136, p. 107556, 2022, doi: 10.1016/j.ijepes.2021.107556.
- [17] S. Ghosh and N. Senroy, "The localness of electromechanical oscillations in power systems," *International Journal of Electrical Power & Energy Systems*, vol. 42, no. 1, pp. 306-313, Jan. 2012, doi: 10.1016/j.ijepes.2012.04.004.
- [18] Y. Li, D. Yang, Y. Liu, Y. Cao, and C. Rehtanz, "Theoretical Foundation of Low-Frequency Oscillations," in *Interconnected Power Systems: Wide-Area Dynamic Monitoring and Control Applications*, Heidelberg, Germany: Springer, 2016, pp. 13-37, doi: 10.1007/978-3-662-48627-6_2.
- [19] P. W. Sauer, M. A. Pai, and J. H. Chow, *Power System Dynamics and Stability: With Synchrophasor Measurement and Power System Toolbox*, 2nd ed., Hoboken, NJ, USA: Wiley-IEEE Press, 2017.
- [20] I. El Karaoui, M. M. Maaroufi, and B. Bossoufi, "Robust power control methods for wind turbines using DFIG-generator," *International Journal of Power Electronics and Drive System (IJPEDS)*, vol. 10, no. 4, pp. 2101-2117, Dec. 2019, doi: 10.11591/ijpeds.v10.i4.pp2101-2117.
- [21] A. A. Shaimaa Shukri and L. A. Alnabi, "Enhancement transient stability of wind power system of doubly-fed induction generator using STATCOM and PI controller," *International Journal of Power Electronics and Drive System (IJPEDS)*, vol. 10, no. 4, pp. 1977-1985, Dec. 2019, doi: 10.11591/ijpeds.v10.i4.pp1977-1985.
- [22] J. C. Muñoz and C. A. Cañizares, "Comparative stability analysis of DFIG-based wind farms and conventional synchronous generators," in *2011 IEEE/PES Power Systems Conference and Exposition*, 2011, pp. 1-7, doi: 10.1109/PSCE.2011.5772545.
- [23] J. M. Akanto, M. K. Islam, E. Jahan, M. R. Hazari, M. A. Mannan, and M. A. Rahman, "Dynamic analysis of grid-connected hybrid wind farm," *International Journal of Power Electronics and Drive System (IJPEDS)*, vol. 14, no. 2, pp. 1230-1237, 2023, doi: 10.11591/ijpeds.v14.i2.pp1230-1237.
- [24] A. R. Al-Roomi, *Power Flow Test Systems Repository*, Halifax, Canada: Dalhousie University, 2015. [Online]. Available: <https://al-roomi.org/power-flow> (accessed Jan. 20, 2023).
- [25] F. Milano, "An open-source power system analysis toolbox," in *IEEE Transactions on Power Systems*, vol. 20, no. 3, pp. 1199-1206, 2005, doi: 10.1109/TPWRS.2005.851911.

BIOGRAPHIES OF AUTHORS



Khaled Kouider    was born on May 14, 1991, in Bechar, Algeria. He received a Master's degree in Electrical Networks from Tahri Mohamed University in Bechar, Algeria in July 2015. He is a member of the Control, Analysis and Optimization of the Electro-Energetic Systems (CAOSEE) Laboratory since December 2015. His areas of interest include wind power integration in power systems, electrical technology, power electronics, power system analysis, operation and control, and power system dynamics and stability. He can be contacted at email: khouiledkhaled@gmail.com.



Abdelkader Bekri    was born on December 4, 1965, in Bechar. He obtained his state engineer degree in electrical engineering from the University of Sciences and Technology of Oran (USTO), Algeria. He also holds an M.Sc. degree from the Electrical Engineering Institute of the Tahri Mohamed University, Bechar, Algeria, and a Ph.D. degree from the same institute. Currently, he is a professor of electrical engineering at the University of Tahri Mohamed, Bechar, Algeria. He can be contacted at email: bekri.abdelkader@univ-bechar.dz.